J. Fluid Mech. (1988), *vol.* 195, *pp.* 257–280
Printed in Great Britain

Dynamic simulation of hydrodynamically interacting suspensions

By JOHN F. BRADY†, RONALD J. PHILLIPS‡, JULIA C. LESTER† AND GEORGES BOSSIS‖

† Department of Chemical Engineering, California Institute of Technology, Pasadena, CA 91125, USA

‡ Department of Chemical Engineering, Massachusetts Institute of Technology, Cambridge, MA 02139, USA

‖ Laboratoire de Physique de la Matière Condensée, Université de Nice, Parc Valrose, 06034 Nice Cedex, France

(Received 8 October 1987)

A general method for computing the hydrodynamic interactions among an infinite suspension of particles, under the condition of vanishingly small particle Reynolds number, is presented. The method follows the procedure developed by O'Brien (1979) for constructing absolutely convergent expressions for particle interactions. For use in dynamic simulation, the convergence of these expressions is accelerated by application of the Ewald summation technique. The resulting hydrodynamic mobility and/or resistance matrices correctly include all far-field non-convergent interactions. Near-field lubrication interactions are incorporated into the resistance matrix using the technique developed by Durlofsky, Brady & Bossis (1987). The method is rigorous, accurate and computationally efficient, and forms the basis of the Stokesian-dynamics simulation method. The method is completely general and allows such diverse suspension problems as self-diffusion, sedimentation, rheology and flow in porous media to be treated within the same formulation for any microstructural arrangement of particles. The accuracy of the Stokesian-dynamics method is illustrated by comparing with the known exact results for spatially periodic suspensions.

1. Introduction

Determining the interactions among a large collection of hydrodynamically interacting particles at zero particle Reynolds number is complicated by the long-range nature of the interactions. The fluid velocity disturbance caused by a particle on which a net external force acts decays as $1/r$, where r is the distance from the particle. A large collection of such forced particles, i.e. an infinite sedimenting suspension, results in a severely non-convergent sum of interactions; the velocity of a test particle diverges as R^2, where R is the size of the system. If the particles are fixed in space, as in a porous medium, rather than having a prescribed force, the long-range interactions actually change the fundamental character of the velocity disturbance caused by a particle, resulting in a screening of hydrodynamic interactions (Brinkman 1947; Saffman 1973; Howells 1974; Hinch 1977; Rubinstein 1986; Durlofsky & Brady 1987). Similar, but less severe, divergences occur if the particles are force free. The origin, significance and interpretation of these convergence difficulties are now well understood, and several procedures have been

devised for overcoming them, resulting in well-posed, absolutely convergent expressions for sedimentation velocities, bulk stresses, etc. (Batchelor 1972; Batchelor & Green 1972; Jeffrey 1973; Hinch 1977; O'Brien 1979).

When one attempts to study the behaviour of suspensions through dynamic simulation, however, most of these methods are not suitable because they preaverage the interactions. In a simulation, absolutely convergent expressions are needed for particle interactions for each and every configuration, not just expressions that are correct on average. The method proposed by O'Brien is the most convenient for adaptation to simulation, and we have been advocating its use since the original development of our simulation method for hydrodynamically interacting particles, which we have called Stokesian dynamics (Bossis & Brady 1984, 1987; Brady & Bossis 1985, 1988). O'Brien's method gives an *exact* procedure for treating the long-range hydrodynamic interactions, with the result that such diverse suspension properties as sedimentation, permeability and rheology can all be treated with the same framework for any arrangement of particles. It is the purpose of this paper to present the modifications we have made to O'Brien's original method and to show how it can be used with dynamic simulation to provide a rigorous foundation for studying hydrodynamic interactions in suspensions.

In O'Brien's method we start from an integral representation for the solution to Stokes' equations for the velocity field $\boldsymbol{u}(\boldsymbol{x})$ at a point $\boldsymbol{x}$ in terms of integrals of the force distribution on the particle surfaces and an integral over a mathematical surface of large radius. In this 'macroscopic boundary' integral, the stresses and velocities may be replaced by their *suspension average* values, and manipulation of this integral results in convergent expressions for the fluid and particle velocities. These expressions take the form of a discrete sum over the force densities of the individual particles minus a volume integral of a continuous distribution of force moments, i.e. a continuous distribution of monopoles, dipoles and quadrupoles. In the case where the average force (monopole) acting on the particles is non-zero, the integrals deriving from this mathematical surface represent a 'backflow' of fluid relative to zero-volume-flux axes. Thus, expressions relating the particle velocities to this average result; indeed, it is the velocity relative to the back flow that is the physically significant quantity, not its absolute value.

The convergent expressions obtained by this procedure can be used directly in theoretical studies of suspension properties; they reproduce the formulae used by Batchelor (1974) and others. For use in dynamic simulation, however, both the accuracy and computational efficiency can be improved by replicating a finite number of particles periodically throughout the suspension volume. With the use of periodic boundary conditions, the sum of particle interactions becomes a so-called lattice sum, and the Ewald (1921) summation technique, as first employed by Beenakker (1986) to hydrodynamic interactions, can be used to accelerate convergence of the lattice sums.

The Ewald sums not only improve accuracy, they (or an equivalent procedure) are essential when periodic boundary conditions are used. The central element needed to compute particle motion is the hydrodynamic mobility matrix, which relates particle velocities to the forces all the particles exert on the fluid. Because of the dissipative nature of the Stokes' equations, the mobility matrix must be positive definite. Mobility matrices constructed with periodic boundary conditions without Ewald sums, however, lose positive definiteness at quite low values of the volume fraction ($\phi \approx 0.05$), resulting in completely aphysical behaviour. This important aspect has

been noticed by researchers conducting dynamic simulation of suspensions (Dickinson 1985), but previous attempts to remedy this situation have not met success (Smith, Snook & van Megen 1987). We shall see that the method developed here correctly includes the physics of the long-range hydrodynamic interactions, and the mobility matrices never lose positive definiteness.

The interactions rendered convergent by O'Brien's method and calculated by Ewald sums are all long-range or far-field interactions; the near-field physics is unaffected. To accurately determine particle interactions in a suspension, particularly a concentrated suspension, however, both the far- and the near-field physics must be modelled correctly. The short-range lubrication forces result in, among other effects, the relative motion of two particles going to zero as the particle surfaces approach one another, and these interactions can be paramount in determining dense suspension behaviour. The lubrication forces can be conveniently (accurately and efficiently) included in the hydrodynamic resistance matrix (the inverse of the mobility matrix) through the method developed by Durlofsky, Brady & Bossis (1987). The final product is a convergent hydrodynamic mobility and/or resistance matrix that accurately models both the far- and near-field interactions.

In §2 we develop the general method for simulating an infinite suspension of hydrodynamically interacting particles. The correctness and accuracy of this method are illustrated in §3 where we compare our Stokesian-dynamics simulation results with the exact behaviour for spatially periodic suspensions. We shall see that the simulation results agree well with the sedimentation velocity and permeability of cubic arrays calculated by Zick & Homsy (1982) from the dilute limit up to close packing. For the shear viscosity of cubic arrays our results are in excellent agreement with the exact calculations of Zuzovsky, Adler & Brenner (1983) and Nunan & Keller (1984). We conclude in §4 with a discussion of the extension of the method to non-hydrodynamic systems, particularly electrostatic or thermal conductivity problems, where the same approach is applicable and has actually been carried out (Bonnecaze 1987).

2. Method

In this section we present a general method for constructing hydrodynamic interactions among N particles suspended in a volume V under conditions such that the particle Reynolds number is small, so that the fluid motion is governed by Stokes' equations. First, convergent expressions for the hydrodynamic interactions in the infinite suspension or 'thermodynamic' limit $N \to \infty$, $V \to \infty$, keeping $n = N/V$ fixed, are constructed. In this analysis we follow closely the original presentation by O'Brien, with the exception of changing to the Stokes' flow case rather than the thermal conductivity problem where Laplace's equation holds, and the reader is referred to O'Brien (1979) for a more detailed discussion. Second, we recast the convergent expressions into lattice sums by periodically replicating a finite number of particles throughout space and use the Ewald summation technique to accelerate the convergence of these sums. And third, we discuss how to include the near-field lubrication interactions in the hydrodynamic mobility tensors.

2.1. *Convergent hydrodynamic interactions*

Using the Green function for Stokes' equations (Ladyzhenskaya 1963), the velocity field $\boldsymbol{u}(\boldsymbol{x})$ at any point $\boldsymbol{x}$ in the fluid can be written in terms of integrals of the force

distribution on the surfaces of the particles and an integral over a mathematical surface Γ' of large radius lying entirely within the fluid:

$$u_i(\boldsymbol{x}) = -\frac{1}{8\pi\eta}\sum_{\alpha=1}^{N}\int_{S_\alpha} J_{ij}(\boldsymbol{x}-\boldsymbol{y})\,\sigma_{jk}(\boldsymbol{y})\,n_k(\boldsymbol{y})\,\mathrm{d}S_y$$

$$-\frac{1}{8\pi\eta}\int_{S_{\Gamma'}}[J_{ij}(\boldsymbol{x}-\boldsymbol{y})\,\sigma_{jk}(\boldsymbol{y})+2\eta\,K_{ijk}(\boldsymbol{x}-\boldsymbol{y})\,u_j(\boldsymbol{y})]\,n_k\,\mathrm{d}S_y. \quad (2.1)$$

Here, J_{ij} is the Green function for Stokes' flow

$$J_{ij}(\boldsymbol{r}) = \frac{\delta_{ij}}{r}+\frac{r_i r_j}{r^3}, \quad (2.2)$$

and

$$K_{ijk}(\boldsymbol{r}) = -3\frac{r_i r_j r_k}{r^5}. \quad (2.3)$$

We define δ_{ij} as the unit isotropic tensor, η as the viscosity of the suspending fluid, and $\boldsymbol{\sigma}$ as the fluid stress tensor:

$$\sigma_{ij} = -p\delta_{ij}+2\eta e_{ij}, \quad (2.4)$$

where p is the pressure, and $e_{ij} = \frac{1}{2}[\nabla_i u_j+\nabla_j u_i]$ is the rate-of-strain tensor. We note that $\boldsymbol{r} = \boldsymbol{x}-\boldsymbol{y}$, with $\boldsymbol{y}$ a point on the surface, and $\boldsymbol{n}$ is the outer normal to the surfaces, i.e. pointing into the volume V containing the N particles.

Equation (2.1) is an exact formulation for rigid particles. (Recall that for rigid particles $\int_{S_\alpha} K_{ijk}\,u_j\,n_k\,\mathrm{d}S = 0$.) No divergences occur because we have a finite region bounded by the surface Γ'. This is an arbitrary surface immersed in an unbounded statistically homogeneous suspension, i.e. the suspension continues outside of Γ'. If the radius R of this surface is taken to be very large (with the origin located near the field point $\boldsymbol{x}$), the variation in $\boldsymbol{J}$ and $\boldsymbol{K}$ will be small over a surface element $\mathrm{d}S_{\Gamma'}$ that passes through the fluid and around many particles. Thus, in the integrand of the second integral we may replace σ and $\boldsymbol{u}$ by averages. This is facilitated by first transforming from Γ' to a smooth macroscopic surface Γ that cuts both fluid and particles; the averages thus formed are *suspension averages* – fluid and particle phase averages. Because the local normal to the surface Γ' varies on the particle scale, in addition to averages of $\boldsymbol{\sigma}$ and $\boldsymbol{u}$, the particles generate a quadrupolar contribution upon reduction from Γ' to Γ. Following a procedure similar to that used by Glendinning & Russel (1982) it may be shown that

$$\int_{S_{\Gamma'}}[J_{ij}\,\sigma_{jk}+2\eta\,K_{ijk}\,u_j]\,n_k\,\mathrm{d}S_y = \int_{S_\Gamma}\{J_{ij}\langle\sigma_{jk}\rangle\,n_k+2\eta\,K_{ijk}\langle u_j\rangle\,n_k$$

$$-n\nabla_k J_{ij}\langle Q'_{klj}\rangle\,n_l\}\,\mathrm{d}S_y. \quad (2.5)$$

Here, $\langle\boldsymbol{\sigma}\rangle$ and $\langle\boldsymbol{u}\rangle$ are the suspension-average hydrodynamic stress and velocity, and $\langle\boldsymbol{Q}'\rangle$ is the average quadrupole density of the particles. The quadrupole of particle α is defined by

$$Q'^{\alpha}_{klj} \equiv -\frac{1}{2}\int_{S_\alpha}(y_k-x^\alpha_k)\,(y_l-x^\alpha_l)\,\sigma_{jm}\,n_m\,\mathrm{d}S_y, \quad (2.6)$$

where $\boldsymbol{x}^\alpha$ is the 'centre' of particle α. The derivative of $\boldsymbol{J}$ in the quadrupole integral is with respect to $\boldsymbol{y}$.

The use of the suspension-average quantities is the key step and the only

assumption made in O'Brien's method. In a statistically homogeneous medium $\langle \boldsymbol{\sigma} \rangle$ and $\langle \boldsymbol{u} \rangle$ are either constants or linear functions of position, coming from the average pressure in $\langle \boldsymbol{\sigma} \rangle$ and a linear shear flow in $\langle \boldsymbol{u} \rangle$, while $\langle \boldsymbol{Q}' \rangle$ is constant. With (2.5) equation (2.1) becomes

$$u_i(\boldsymbol{x}) = -\frac{1}{8\pi\eta} \sum_{\alpha=1}^{N} \int_{S_\alpha} J_{ij}\, \sigma_{jk}\, n_k \, \mathrm{d}S_y - \frac{1}{8\pi\eta} \int_{S_\Gamma} \{J_{ij} \langle \sigma_{jk} \rangle n_k + 2\eta K_{ijk} \langle u_j \rangle n_k - n \nabla_k J_{ij} \langle Q'_{klj} \rangle n_l\} \, \mathrm{d}S_y. \quad (2.7)$$

In the sum over α, only the particle surfaces that lie within Γ are included.

Equation (2.7) is the key result of O'Brien's method and leads to convergent expressions for the fluid velocity at any point $\boldsymbol{x}$, as well as for the hydrodynamic interactions among the particles. By use of the divergence theorem, the macroscopic boundary integral over Γ can be converted into a volume integral of uniform distributions of average forces (monopoles), dipoles, and quadrupoles. At large distances from the field point $\boldsymbol{x}$, we may expand the force density on the surface of a particle α in moments, and the sum over α in (2.7) will approximate a volume integral of a continuous distribution of average monopoles, dipoles and quadrupoles. Thus, the sum and integral will cancel, leaving a finite result for the velocity. Note that the velocity disturbance caused by a quadrupole decays as $1/r^3$, while the next moment in the expansion of the particle surface force density, the octupole, creates a disturbance that decays as $1/r^4$; thus, the sum over the octupoles and higher moments is absolutely convergent. This is the essence of the method.

To complete the derivation we need to relate the average hydrodynamic stress $\langle \boldsymbol{\sigma} \rangle$ to the rate of strain, and by doing so introduce the particle contributions to the average stress. At any point within the fluid Stokes' equations can be written as

$$\nabla \cdot \boldsymbol{\sigma} = 0, \quad (2.8)$$

and within the solid particles we have

$$\nabla \cdot \boldsymbol{\sigma} = -\boldsymbol{f}, \quad (2.9)$$

where $\boldsymbol{f}$ is the external force per unit volume acting on the particles. The most common example for this body force is gravity; here, $\boldsymbol{f} = \boldsymbol{F}^g / V_P$, where $\boldsymbol{F}^g$ is the net (with the buoyancy removed) force of gravity acting on a particle of volume V_P. A volume or ensemble average of (2.8) and (2.9) results in

$$\nabla \cdot \langle \boldsymbol{\sigma} \rangle = -n \langle \boldsymbol{F} \rangle, \quad (2.10)$$

where

$$\langle \boldsymbol{F} \rangle = \frac{1}{N} \sum_{\alpha} \int_{V_\alpha} \boldsymbol{f}^\alpha \, \mathrm{d}V$$

is the average net external force acting on the particles, which equals the net force the particles exert on the fluid.

An expression for the average stress can be obtained by following the arguments of Landau & Lifshitz (1959) and Batchelor (1970); the result is

$$\langle \sigma_{ij} \rangle = -\langle p \rangle \delta_{ij} + 2\eta \langle e_{ij} \rangle - n\{\langle S_{ij} \rangle + \langle \mathscr{L}_{ij} \rangle\}, \quad (2.11)$$

where

$$\langle S_{ij} \rangle = \frac{1}{N} \sum_{\alpha=1}^{N} S_{ij}^\alpha, \quad \langle \mathscr{L}_{ij} \rangle = \frac{1}{N} \sum_{\alpha=1}^{N} \mathscr{L}_{ij}^\alpha$$

and the particle stresslet and rotlet densities, $\boldsymbol{S}^\alpha$ and $\mathscr{L}^\alpha$ respectively, are given by

$$S_{ij}^\alpha \equiv -\frac{1}{2}\int_{S_\alpha} [\sigma_{ik}(y_j - x_j^\alpha) + \sigma_{jk}(y_i - x_i^\alpha) - \tfrac{2}{3}\delta_{ij}\sigma_{lk}(y_l - x_l^\alpha)] n_k \, \mathrm{d}S_y, \tag{2.12}$$

and

$$\mathscr{L}_{ij}^\alpha \equiv -\frac{1}{2}\int_{S_\alpha} [\sigma_{ik}(y_j - x_j^\alpha) - \sigma_{jk}(y_i - x_i^\alpha)] n_k \, \mathrm{d}S_y. \tag{2.13}$$

$\mathscr{L}_{ij}^\alpha$ can also be related to the external torque, $\boldsymbol{L}^\alpha$, the particle exerts on the fluid by

$$L_i^\alpha = \epsilon_{ijk}\mathscr{L}_{jk}^\alpha, \tag{2.14}$$

where

$$L_i^\alpha = -\int_{S_\alpha} \epsilon_{ijk}\sigma_{jl}(y_k - x_k^\alpha) n_l \, \mathrm{d}S_y. \tag{2.15}$$

In a statistically homogeneous medium $\nabla\cdot\langle\boldsymbol{S}\rangle = \nabla\cdot\langle\mathscr{L}\rangle = 0$, and (2.10)–(2.11) can be used to write the pressure $\langle p\rangle$ as

$$\langle p\rangle = n\langle F_i\rangle (x_i - x_i^0), \tag{2.16}$$

where $\boldsymbol{x}^0$ is an arbitrary reference position at which we set the average pressure to zero. Equation (2.16) is just a statement of the macroscopic hydrostatic balance between the average pressure and the average force the particles exert on the fluid.

We can make use of the divergence theorem to rewrite the surface integral over Γ in (2.7) as

$$\begin{aligned} &+\frac{1}{8\pi\eta}\int_{V'} \nabla_k[J_{ij}\langle\sigma_{jk}\rangle + 2\eta K_{ijk}\langle u_j\rangle - n\nabla_l J_{ij}\langle Q'_{klj}\rangle] \, \mathrm{d}V_y \\ &-\frac{1}{8\pi\eta}\int_{S_\epsilon} [J_{ij}\langle\sigma_{jk}\rangle n_k + 2\eta K_{ijk}\langle u_j\rangle n_k - n\nabla_k\langle Q'_{klj}\rangle n_l] \, \mathrm{d}S_y, \end{aligned} \tag{2.17}$$

where S_ϵ is a spherical surface of radius ϵ surrounding the field point $\boldsymbol{x}$, and V' is the volume between S_Γ and S_ϵ. Making use of (2.11) and (2.16), the volume integral in (2.17) becomes

$$-\frac{n}{8\pi\eta}\int_{V'} \{J_{ij}\langle F_j\rangle + R_{ij}\langle L_j\rangle + K_{ijk}\langle S_{jk}\rangle + \nabla_k\nabla_l J_{ij}\langle Q'_{klj}\rangle\} \, \mathrm{d}V_y, \tag{2.18}$$

where

$$R_{ij}(r) = \epsilon_{ijk}\frac{r_k}{r^3} = \epsilon_{lkj}\tfrac{1}{4}(\nabla_k J_{il} - \nabla_l J_{ik}) \tag{2.19}$$

is the propagator (or Green function) for a point torque. Because $\langle S_{jk}\rangle$ is symmetric and traceless, K_{ijk} in (2.18) can be set equal to $\frac{1}{2}(\nabla_k J_{ij} + \nabla_j J_{ik})$, the propagator for a point stresslet. Finally, taking the limit as the surface S_ϵ shrinks to the point $\boldsymbol{x}$, the volume V' may be replaced by V, and the surface integral over S_ϵ becomes

$$-\frac{1}{8\pi\eta}\int_{S_\epsilon} [\cdot] \, \mathrm{d}S \sim \langle u_i(\boldsymbol{x})\rangle + \frac{2n}{15\eta}[2\langle Q'_{jji}\rangle - \langle Q'_{ijj}\rangle]. \tag{2.20}$$

Combining (2.17), (2.18) and (2.20), equation (2.7) becomes

$$u_i(\boldsymbol{x})-\langle u_i(\boldsymbol{x})\rangle = \frac{2n}{15\eta}[2\langle Q'_{jji}\rangle-\langle Q'_{iij}\rangle]-\frac{1}{8\pi\eta}\sum_{\alpha=1}^{N}\int_{S_\alpha} J_{ij}\,\sigma_{jk}\,n_k\,\mathrm{d}S_y$$

$$-\frac{n}{8\pi\eta}\int_V \{J_{ij}\langle F_j\rangle + R_{ij}\langle L_j\rangle + K_{ijk}\langle S_{jk}\rangle + \nabla_k\nabla_l J_{ij}\langle Q'_{klj}\rangle\}\,\mathrm{d}V_y. \quad (2.21)$$

Equation (2.21) is the desired result – an absolutely convergent expression for the fluid velocity relative to the suspension average $\langle \boldsymbol{u}\rangle$. We may now let the radius R of the volume V tend to infinity because the sum and the integral will cancel, leaving a finite result. It is quite natural that relative velocities appear, as the motion must be Galilean invariant. The macroscopic boundary integral contributes the volume distributions of monopoles ($\langle \boldsymbol{F}\rangle$), dipoles ($\langle \boldsymbol{L}\rangle$ and $\langle \boldsymbol{S}\rangle$, the antisymmetric and symmetric parts, respectively) and quadrupoles ($\langle \boldsymbol{Q}'\rangle$). Expanding the particle force densities in similar moments will show that (2.21) is indeed absolutely convergent.

Equation (2.21) can perhaps be made more familiar if we consider a suspension of point-force particles sedimenting due to gravity. In this case, $\langle \boldsymbol{L}\rangle = \langle \boldsymbol{S}\rangle = 0$, and we shall see below that $\langle \boldsymbol{Q}'\rangle$ is directly related to the finite size of the particles. Hence, (2.21) becomes

$$u_i(\boldsymbol{x})-\langle u_i(\boldsymbol{x})\rangle = \frac{1}{8\pi\eta}\sum_{\alpha=1}^{N} J_{ij}(x-x^\alpha)\,F_j^\alpha - \frac{n}{8\pi\eta}\int J_{ij}\langle F_j\rangle\,\mathrm{d}V, \quad (2.22)$$

where the force a particle exerts on the fluid is given by

$$F_i^\alpha \equiv -\int_{S_\alpha}\sigma_{ij}\,n_j\,\mathrm{d}S. \quad (2.23)$$

Physically, the integral represents a 'backflow' of fluid, relative to zero-volume-flux axes $\langle \boldsymbol{u}\rangle = 0$, caused by the macroscopic pressure gradient that balances the excess weight, $\langle \boldsymbol{F}\rangle \neq 0$, of the particles. Expressions analogous to (2.22) can be found in previous analyses of convergence problems in suspensions.

Although (2.21) gives a convergent expression for the fluid velocity, we are often most interested in the motion of the particles rather than the fluid. Furthermore, unlike the force and torque, which are often prescribed in a problem, the stresslet and quadrupole densities (and higher moments) are not given, but must be found as part of the problem. To obtain a complete set of equations for the particle interactions, equations analogous to (2.21) can be derived from (2.7) for $\nabla_j u_i$, $\nabla_j\nabla_k u_i$, etc., and these can be used in conjunction with Faxén formulae to determine the particle velocities, and so on.

We restrict our attention now to identical spherical particles of radii a for which the Faxén formulae are simple (cf. Durlofsky *et al.* 1987), but the general approach can also be used for a distribution of particle sizes and for non-spherical particles. It will prove convenient to define an irreducible quadrupole moment density, $\boldsymbol{Q}^\alpha$, of particle α, because the trace of $\boldsymbol{Q}'^\alpha$ is proportional to the total force. Thus,

$$Q^\alpha_{klj} \equiv Q'^\alpha_{klj} - \frac{a^2}{6}F_j^\alpha\,\delta_{kl}, \quad (2.24)$$

and $Q^\alpha_{kkj} = 0$.

Repeating the analysis that lead to (2.21) for the velocity gradients and using the

Faxén laws, the following equations for the particle velocities, etc. may be derived:

$$U_i^\alpha - \langle u_i(\boldsymbol{x}^\alpha)\rangle = \phi\frac{\langle F_i\rangle}{6\pi\eta a} - \tfrac{3}{5}\phi\frac{\langle Q_{ijj}\rangle}{6\pi\eta a^3} + \frac{F_i^\alpha}{6\pi\eta a} - \frac{1}{8\pi\eta}\sum_{\beta\neq\alpha}\int_{S_\beta}\left(1+\frac{a^2}{6}\nabla^2\right)J_{ij}\,\sigma_{jk}\,n_k\,\mathrm{d}S_y$$

$$-\frac{n}{8\pi\eta}\int_V\left\{\left(1+\frac{a^2}{3}\nabla^2\right)J_{ij}\langle F_j\rangle + R_{ij}\langle L_j\rangle + K_{ijk}\langle S_{jk}\rangle + \nabla_k\nabla_l J_{ij}\langle Q_{klj}\rangle\right\}\mathrm{d}V_y, \quad (2.25)$$

$$\Omega_i^\alpha - \langle\omega_i(\boldsymbol{x}^\alpha)\rangle = \phi\frac{\langle L_i\rangle}{8\pi\eta a^3} + \frac{L_i^\alpha}{8\pi\eta a^3} - \frac{1}{8\pi\eta}\sum_{\beta\neq\alpha}\int_{S_\beta}\tfrac{1}{2}\epsilon_{ijk}\nabla_j J_{kl}\,\sigma_{lm}\,n_m\,\mathrm{d}S_y,$$

$$-\frac{n}{8\pi\eta}\int_V\tfrac{1}{2}\epsilon_{ijk}\nabla_j\{J_{kl}\langle F_l\rangle + R_{kl}\langle L_l\rangle + K_{klm}\langle S_{lm}\rangle\}\,\mathrm{d}V_y, \quad (2.26)$$

$$0 - \langle e_{ij}(\boldsymbol{x}^\alpha)\rangle = -\phi\frac{\langle S_{ij}\rangle}{\frac{20}{3}\pi\eta a^3} + \frac{S_{ij}^\alpha}{\frac{20}{3}\pi\eta a^3} - \frac{1}{8\pi\eta}\sum_{\beta\neq\alpha}\int_{S_\beta}\left(1+\frac{a^2}{10}\nabla^2\right)\nabla_j^{sym}J_{ik}\,\sigma_{kl}\,n_l\,\mathrm{d}S_y$$

$$-\frac{n}{8\pi\eta}\int_V\nabla_j^{sym}\{J_{ik}\langle F_k\rangle + R_{ik}\langle L_k\rangle + K_{ikl}\langle S_{kl}\rangle\}\,\mathrm{d}V_y, \quad (2.27)$$

and

$$0 = \tfrac{1}{10}\phi\frac{\langle F_m\rangle}{6\pi\eta a}\{\delta_{km}\delta_{jl} + \delta_{lm}\delta_{kj} - \tfrac{2}{3}\delta_{kl}\delta_{jm}\} - \frac{Q_{klj}^\alpha}{6\pi\eta a^3}$$

$$-\frac{1}{8\pi\eta}\sum_{\beta\neq\alpha}\int_{S_\beta}B_{kl}J_{jm}\,\sigma_{mn}\,n_n\,\mathrm{d}S_y - \frac{n}{8\pi\eta}\int_V B_{kl}J_{jm}\langle F_m\rangle\,\mathrm{d}V_y. \quad (2.28)$$

In these equations, $\phi = \frac{4}{3}\pi a^3 n$ is the volume fraction of particles, $\langle\omega_i\rangle = \frac{1}{2}\epsilon_{ijk}\nabla_j\langle u_k\rangle$ is the angular velocity of the bulk suspension, the operator ∇_j^{sym} acting on a vector v_i is defined by $\nabla_j^{sym}v_i \equiv \frac{1}{2}(\nabla_j v_i + \nabla_i v_j)$, and $B_{kl}J_{jm}$ is a second-order differential operator giving the irreducible quadrupole density of a particle due to a point force. The detailed form of $B_{kl}J_{jm}$ can be found in Mazur & van Saarloos (1982, cf. their equation (6.18)), but it will not be needed here. Note that there is no 'kinematic' term on the left-hand side of (2.28) because $\boldsymbol{\nabla\nabla u}$ is zero within a rigid particle and $\boldsymbol{\nabla\nabla}\langle\boldsymbol{u}\rangle = 0$ for linear bulk flows. A quadratic bulk flow can only be produced by the presence of actual physical boundaries and these would have to be explicitly included in the formulation (cf. Durlofsky 1986; Durlofsky & Brady 1988).

Equations (2.25)–(2.28) give the desired result of absolutely convergent expressions for particle interactions in a fluid suspension. The development could be continued to higher moments, but no additional convergence problems arise, so a higher-order development is unnecessary. Indeed, even the quadrupoles are only marginally necessary as they are induced by particle interactions; that is, for an isolated sphere $\boldsymbol{Q}$ is zero. The most important contribution to the quadrupole density is the 'mean-field' part proportional to $\langle\boldsymbol{F}\rangle$ coming from the macroscopic boundary integral. In order to reduce the number of unknowns or degrees of freedom necessary to simulate particle behaviour, we shall approximate the quadrupole moment density of each and every particle by its mean value, i.e.

$$\frac{Q_{klj}^\alpha}{6\pi\eta a^3} \approx \tfrac{1}{10}\phi\frac{\langle F_m\rangle}{6\pi\eta a}\{\delta_{km}\delta_{jl} + \delta_{lm}\delta_{kj} - \tfrac{2}{3}\delta_{kl}\delta_{jm}\}. \quad (2.29)$$

It will be shown in §3 that this approximation is actually rather good, and the additional accuracy provided by retaining the full quadrupole expression (2.28) is not worth the additional computational costs. We shall use this mean-field quadrupole in (2.25) in the coupling between translational velocities and forces only. It is not used in conjunction with the higher moments. The form of (2.29) results in a very convenient incorporation into (2.25): the constant term $-\frac{3}{5}\phi\langle Q_{ijj}\rangle/6\pi\eta a^3 = -\frac{1}{5}\phi^2\langle F_i\rangle/6\pi\eta a$, and $\frac{1}{3}a^2\nabla^2$ in the backflow integral (and the particle surface integrals) can be replaced with $\frac{1}{3}a^2(1-\frac{1}{5}\phi)\nabla^2$. With this mean-field quadrupole approximation (2.28) is no longer needed, and we shall only be concerned with forces, torques and stresslets. (Note that if one wished to make a simple improvement on (2.29) by smoothing out the discrete sum in (2.28), the resulting contribution, for a point-force isotropic suspension, would be of the form $\phi\int[g(r)-1]B_{kl}J_{jm}F_m\,\mathrm{d}V$, which is zero from angular integration. Here, $g(r)$ is the pair-distribution function.)

Finally, we note that for a sedimenting suspension ($\langle \boldsymbol{S}\rangle = \langle \boldsymbol{L}\rangle = 0$), (2.25) reduces to the expression used by Batchelor (1972) for determining the sedimentation velocity of a random suspension. Similarly, (2.27) is the starting point for determining the bulk stress in a suspension of force- and torque-free particles in the analysis of Batchelor & Green (1972).

2.2. *Ewald sums*

Expressions (2.25)–(2.27) are quite useful as a starting point for theoretical studies of suspension problems, but they are not yet in a form suitable for dynamic simulation. The sum and the integral in these expressions both increase with the size R of the volume, but their difference is finite and is what is needed. In simulation many particles may be needed before the sum approximates a continuous distribution and convergence is obtained. In order to reduce the number of particles needed and to accelerate the convergence of expressions like (2.25)–(2.27), we take a finite number N_1 of particles and replicate them periodically within the volume V. This periodic sum can be efficiently computed with a summation technique due to Ewald (1921). To illustrate the procedure, we shall first consider a suspension of point forces only.

For point forces, (2.25) reduces to (2.22) with $\boldsymbol{u}(\boldsymbol{x})$ replaced by $\boldsymbol{U}^\alpha$. Thus, for the translational velocity of particle α at the centre of its periodic cell, (2.25) becomes

$$U_i^\alpha - \langle u_i(\boldsymbol{x}^\alpha)\rangle = \frac{1}{8\pi\eta}\sum_\gamma {\sum_{\beta=1}^{N_1}}' J_{ij}(\boldsymbol{x}^\alpha - \boldsymbol{x}^\beta)F_j^\beta - \frac{n}{8\pi\eta}\int_0^\infty J_{ij}\langle F_j\rangle\,\mathrm{d}V, \tag{2.30}$$

where γ labels the periodic cells and the $'$ on the sum indicates that for $\alpha = \beta$ in cell $\gamma = 1$, $\boldsymbol{J}$ is replaced by $4\boldsymbol{I}/(3a)$, giving the correct self-term. α labels an arbitrary particle.

If N_1 were sufficiently large, then the contribution to the αth particle velocity from particles in cells $\gamma > 1$, i.e. outside its own periodic box, would cancel the part of the integral from L to ∞, where L is the size of a periodic box. There would remain, however, a constant from the backflow integral from 0 to L. Because of the slow convergence of the difference between the sum and the integral, N_1 may need to be prohibitively large. Expressions of this type containing so-called lattice sums occur frequently in electrostatic problems, for example in computing the cohesive energy or Madelung constant of an ionic crystal, and can be accelerated using Ewald summations, which rewrite the sum into two rapidly converging parts, one in real space and the other in reciprocal space.

Beenakker (1986) has recently worked out the Ewald sums for $\boldsymbol{J}$ under the assumption that the average force is zero, $\langle \boldsymbol{F} \rangle = 0$, i.e. just the sums in (2.30) with no backflow integral. We shall briefly sketch the Ewald summation of (2.30), following first the analysis of Beenakker when $\langle \boldsymbol{F} \rangle = 0$, and then extending this to the non-zero average-force case. For details of the procedure the reader is referred to Beenakker's excellent two-page paper.

The Ewald sum is affected by noting that $\boldsymbol{J}(\boldsymbol{r})$ may be written as $J_{ij}(\boldsymbol{r}) = (\delta_{ij}\nabla^2 - \nabla_i \nabla_j) r$, from which we may write

$$\tfrac{3}{4} J_{ij}(\boldsymbol{r}) = M^{(1)}_{ij}(\boldsymbol{r}) + M^{(2)}_{ij}(\boldsymbol{r}), \tag{2.31}$$

with

$$M^{(1)}_{ij}(\boldsymbol{r}) = \tfrac{3}{4}(\delta_{ij}\nabla^2 - \nabla_i \nabla_j)(r \operatorname{erfc}(\xi r)), \tag{2.32}$$

$$M^{(2)}_{ij}(\boldsymbol{r}) = \tfrac{3}{4}(\delta_{ij}\nabla^2 - \nabla_i \nabla_j)(r \operatorname{erf}(\xi r)), \tag{2.33}$$

where

$$\operatorname{erfc}(x) = 1 - \operatorname{erf}(x) = 2/\pi^{\frac{1}{2}} \int_x^\infty \exp(-z^2)\, \mathrm{d}z$$

is the complementary error function, and ξ is an arbitrary parameter with units of inverse length that sets the speed of convergence of the sums. The factor of $\frac{3}{4}$ has been introduced for convenience.

With these definitions (2.30) without the backflow integral becomes

$$6\pi\eta U^\alpha_i = F^\alpha_i + \sum_\gamma{}' \sum_{\beta=1}^{N_1} M^{(1)}_{ij}(\boldsymbol{x}^\alpha - \boldsymbol{x}^\beta) F^\beta_j - M^{(2)}_{ij}(\boldsymbol{r}=0) F^\alpha_j + \sum_\gamma \sum_{\beta=1}^{N_1} M^{(2)}_{ij}(\boldsymbol{x}^\alpha - \boldsymbol{x}^\beta) F^\beta_j, \tag{2.34}$$

where the prime on the sum means that the term $\beta = \alpha$ in cell $\gamma = 1$ has been excluded. Note however, that in the $\boldsymbol{M}^{(2)}$ sum this term is included, being cancelled by $\boldsymbol{M}^{(2)}(\boldsymbol{r}=0)$. The first sum in (2.34) converges rapidly in real space, while the second converges rapidly in reciprocal space. Making use of the identity (from the Poisson summation formula)

$$\sum_\gamma g(\boldsymbol{r}_\gamma) = \frac{1}{V} \sum_\lambda g(\boldsymbol{k}_\lambda),$$

where $g(\boldsymbol{k}) = \int \mathrm{e}^{\mathrm{i}\boldsymbol{k}\cdot\boldsymbol{r}} g(\boldsymbol{r})\, \mathrm{d}\boldsymbol{r}$, V is the volume of the periodic cell, and $\boldsymbol{k}_\lambda$ are reciprocal lattice vectors satisfying $\exp(\mathrm{i}\boldsymbol{k}_\lambda \cdot \boldsymbol{r}_\gamma) = 1$, we have

$$\sum_\gamma \sum_{\beta=1}^{N_1} M^{(2)}_{ij}(\boldsymbol{x}^\alpha - \boldsymbol{x}^\beta) F^\beta_j = \frac{1}{V} \sum_\lambda{}' \sum_{\beta=1}^{N_1} \mathrm{e}^{-\boldsymbol{k}_\lambda \cdot (\boldsymbol{x}^\alpha - \boldsymbol{x}^\beta)} M^{(2)}_{ij}(\boldsymbol{k}_\lambda) F^\beta_j, \tag{2.35}$$

where

$$M^2_{ij}(\boldsymbol{k}) = (\delta_{ij} - \hat{k}_i \hat{k}_j)(1 + \tfrac{1}{4}\xi^{-2} k^2 + \tfrac{1}{8}\xi^{-4} k^4)\, 6\pi k^{-2} \exp(-\tfrac{1}{4}\xi^{-2} k^2), \tag{2.36}$$

and $\hat{\boldsymbol{k}} = \boldsymbol{k}/k$. The prime on the sum over λ indicates that the $\boldsymbol{k}_\lambda = 0$ terms are excluded from the sum. The exclusion of these terms is a direct result of the stipulation that $\langle \boldsymbol{F} \rangle = 1/N \sum_{\beta=1}^{N} \boldsymbol{F}^\beta = 0$. To see this note that as $\boldsymbol{k} \to 0$, (2.35) reduces to

$$\frac{1}{V} M^{(2)}_{ij}(\boldsymbol{k} \to 0) \sum_{\beta=1}^{N_1} F^\beta_j. \tag{2.37}$$

This is a key step and one we shall return to when $\langle \boldsymbol{F} \rangle \neq 0$.

$\boldsymbol{M}^{(2)}(\boldsymbol{r}=0)$ can be found from the inverse Fourier transform, giving

$$M_{ij}^{(2)}(\boldsymbol{r}=0) = \frac{1}{(2\pi)^3}\int M_{ij}^{(2)}(\boldsymbol{k})\,\mathrm{d}\boldsymbol{k} = \delta_{ij}\frac{6}{\pi^{\frac{1}{2}}}\xi a, \tag{2.38}$$

Combining together, (2.34) becomes

$$6\pi\eta U_i^\alpha = \left(1-\frac{6}{\pi^{\frac{1}{2}}}\xi a\right)F_i^\alpha + \sum_\gamma{}' \sum_{\beta=1}^{N_1} M_{ij}^{(1)}(\boldsymbol{x}^\alpha-\boldsymbol{x}^\beta)\,F_j^\beta + \frac{1}{V}\sum_\lambda{}' \sum_{\beta=1}^{N_1} M_{ij}^{(2)}(\boldsymbol{k}_\lambda)\,F_j^\beta \cos[\boldsymbol{k}_\lambda\cdot(\boldsymbol{x}^\alpha-\boldsymbol{x}^\beta)]. \tag{2.39}$$

Equation (2.39) is identical to (2.30) (for $\langle\boldsymbol{F}\rangle = 0$) for any value of $\xi > 0$. ξ controls the rate of convergence of the two sums, and Beenakker recommends $\xi = \pi^{\frac{1}{2}}V^{-\frac{1}{3}}$ for simple cubic lattices, giving equal rates of convergence for the two sums.

When the average force is non-zero, the backflow integral cannot be neglected in (2.30), but as we now show it turns out that (2.39) is again the correct result. The $\boldsymbol{k}_\lambda = 0$ terms were removed from the λ-sum in (2.39) because $\Sigma_\beta \boldsymbol{F}^\beta = 0$ in (2.37). When $\langle\boldsymbol{F}\rangle \neq 0$, the backflow integral in (2.30) precisely cancels these $\boldsymbol{k}_\lambda = 0$ terms. To see this, note that we may use the convolution theorem to write the backflow integral as

$$\int J_{ij}\,\mathrm{d}V = \delta(\boldsymbol{k})\hat{J}_{ij}(\boldsymbol{k}), \tag{2.40}$$

where $\delta(\boldsymbol{k})\hat{\boldsymbol{J}}(\boldsymbol{k})$ means the $\lim_{\boldsymbol{k}\to 0}\hat{\boldsymbol{J}}(\boldsymbol{k})$, and the Fourier transform, $\hat{\boldsymbol{J}}$, of $\boldsymbol{J}$ is given by

$$\hat{J}_{ij}(\boldsymbol{k}) = (\delta_{ij}-\hat{k}_i\hat{k}_j)\,6\pi k^{-2} = \lim_{\boldsymbol{k}\to 0} M_{ij}^{(2)}(\boldsymbol{k}).$$

Thus, the reciprocal space sum and the backflow integral become

$$\frac{1}{V}\sum_\lambda\sum_\beta \mathrm{e}^{-\boldsymbol{k}_\lambda\cdot(\boldsymbol{x}^\alpha-\boldsymbol{x}^\beta)}\,M_{ij}^{(2)}(\boldsymbol{k})\,F_j^\beta - n\delta(\boldsymbol{k})\hat{J}_{ij}(\boldsymbol{k})\langle F_j\rangle,$$

which is identical to (2.35). The backflow integral cancels the $\boldsymbol{k}_\lambda = 0$ terms when the average force is non-zero.

Hence, (2.39) is correct whether or not the average force the particles exert on the fluid is zero. This may appear to be a rather surprising result, but there is a simple intuitive argument that shows that it must be true. The coupling between the particle velocities and forces, the mobility matrix, is a purely geometric quantity that describes particle interactions. It cannot depend on the velocities or forces that the particles ultimately have. Therefore, it must be the same whether or not the average force is zero. Said differently, in writing (2.30), or a mobility matrix, the particles do not know whether the forces sum to zero or to a finite average; the particle interactions must be the same in the two cases.

Equation (2.39) gives the correct particle velocities for point-force particles. To include the finite size of the particles and the other non-convergent moments, i.e. the torque, stresslet and quadrupole, we proceed in the same manner as above, but with the complete convergent hydrodynamic interactions (2.25)–(2.27) from O'Brien's method. Just as the backflow integral removed the $\boldsymbol{k}_\lambda = 0$ terms from lattice sum

coupling $\boldsymbol{U}$ and $\boldsymbol{F}$, along with the constants $\phi\langle\boldsymbol{F}\rangle$, $\phi\langle\boldsymbol{S}\rangle$, $\phi\langle\boldsymbol{Q}\rangle$, etc., the backflow integral will remove the $\boldsymbol{k}_\lambda = 0$ terms from all the remaining lattice sums that couple $\boldsymbol{U}$ and $\boldsymbol{L}$, $\boldsymbol{U}$ and $\boldsymbol{S}$, etc. Again, the hydrodynamic interactions are the same whether or not the average force, torque, stresslet or quadrupole are zero.

The Ewald-summed interactions can be most conveniently expressed through the grand mobility matrix $\mathscr{M}$ introduced by Durlofsky *et al.* (1987). The grand mobility matrix relates the translational velocity/rotational velocity/rate of strain of each particle relative to the impressed flow to the force/torque/stresslet of all N particles. Expanding the force density on the surface of each particle in (2.25)–(2.27) in moments, for a finite number, N, of particles in an unbounded fluid we may write (for details see Durlofsky *et al.*)

$$\begin{pmatrix} \boldsymbol{U}-\langle\boldsymbol{u}\rangle \\ -\langle\boldsymbol{e}\rangle \end{pmatrix} = \mathscr{M}\cdot\begin{pmatrix} \boldsymbol{F} \\ \boldsymbol{S} \end{pmatrix}, \tag{2.41}$$

where $\boldsymbol{U}-\langle\boldsymbol{u}\rangle$ is a vector of dimension $6N$ containing the translational and rotational velocities of all N particles relative to the impressed flow $\langle\boldsymbol{u}\rangle$, $-\langle\boldsymbol{e}\rangle$ is a vector of dimension $9N$ that repeats the impressed rate of strain for each particle – all particles experience the same imposed rate of strain, $\boldsymbol{F}$ is a $6N$ vector containing the force and torque exerted by the particles on the fluid, and $\boldsymbol{S}$ of dimension $9N$ contains the particle stresslets. (There are actually only 5 independent components of $\langle\boldsymbol{e}\rangle$ and $\boldsymbol{S}$, because they are symmetric and traceless.) The grand mobility matrix $\mathscr{M}$ is symmetric and positive definite and may be conveniently partitioned into submatrices:

$$\mathscr{M} = \begin{pmatrix} \boldsymbol{M}_{UF} & \boldsymbol{M}_{US} \\ \boldsymbol{M}_{EF} & \boldsymbol{M}_{ES} \end{pmatrix}, \tag{2.42}$$

where the subscripts indicate the coupling of the various components. $\boldsymbol{M}_{UF}$ relates particle velocities to forces and torques, $\boldsymbol{M}_{US}$ relates velocities to stresslets, $\boldsymbol{M}_{EF}$ relates the rate of strain and forces/torques, and $\boldsymbol{M}_{ES}$ relates the rate of strain to stresslets. For the case of N point particles, $\boldsymbol{M}_{UF} = \boldsymbol{J}$, except for the self-term, where $\boldsymbol{I}$ replaces $\boldsymbol{J}$.

Equations (2.41) and (2.42) were written for a finite number of particles in an unbounded fluid. For infinite suspensions, application of the Ewald summations results in a grand mobility matrix of precisely the same form for the N_1 periodically replicated particles. We shall designate this Ewald-summed mobility matrix as $\mathscr{M}^*$. Thus, one need only affix an asterisk to the mobility matrices in (2.41) and (2.42). The impressed flow field is now also properly interpreted as the suspension average flow. The Ewald-summed mobility interactions can be obtained by straightforward, but tedious, calculus along the lines sketched above for point forces; the detailed forms have been placed with the editorial office and may be obtained on request from the editor or the authors.

2.3. *Inclusion of near-field interactions*

The Ewald-summed mobility $\mathscr{M}^*$ includes only the non-convergent, far-field interactions among particles. To include the near-field physics, particularly the near-field lubrication forces, we follow the method of Durlofsky *et al.* (1987) and add these interactions into the grand resistance matrix. The invert of the grand mobility matrix $\mathscr{M}^*$ is the grand resistance matrix $\mathscr{R}^*$ (Ewald summed):

$$\begin{pmatrix} \boldsymbol{F} \\ \boldsymbol{S} \end{pmatrix} = \mathscr{R}^*\cdot\begin{pmatrix} \boldsymbol{U}-\langle\boldsymbol{u}\rangle \\ -\langle\boldsymbol{e}\rangle \end{pmatrix}, \tag{2.43}$$

which may be partitioned as in (2.42) as

$$\mathscr{R}^* = \begin{pmatrix} \boldsymbol{R}^*_{FU} & \boldsymbol{R}^*_{FE} \\ \boldsymbol{R}^*_{SU} & \boldsymbol{R}^*_{SE} \end{pmatrix}. \tag{2.44}$$

As discussed by Durlofsky *et al.* inverting the mobility matrix sums an infinite number of reflected interactions among particles. Thus, the invert of the Ewald-summed mobility matrix sums an infinite number of reflected interactions among an *infinite* number of particles. These reflected interactions reproduce both the screening characteristic of porous media (cf. Durlofsky & Brady 1987) and the effective viscosity of free suspensions. The resistance matrix $\mathscr{R}^*$ still lacks, however, near-field lubrication interactions. Lubrication would only be reproduced upon inversion of the mobility matrix if *all* multipole moments were included. To include lubrication, we introduce it in a pairwise additive fashion. To each element of $(\mathscr{M}^*)^{-1}$ we add the known exact two-sphere resistance interactions (Arp & Mason 1977; Jeffrey & Onishi 1984; Kim & Mifflin 1985), which we shall designate $\mathscr{R}_{2B}$, for two-body resistance matrix. However, part of the two-sphere resistance interactions, the far-field part, has already been included upon the inversion of $\mathscr{M}^*$. Thus, in order not to count these interactions twice, we must subtract off the two-body reflected interactions already contained in $(\mathscr{M}^*)^{-1}$. The matrix composed of these two-body infinite reflection interactions is denoted by $\mathscr{R}^{\infty}_{2B}$, and is found by simply inverting a two-body mobility matrix containing terms to the same order in $1/r$ as in $\mathscr{M}$. Thus, our approximation to the Ewald-summed resistance matrix that contains both near-field lubrication and far-field many-body interactions is

$$\mathscr{R}^* = (\mathscr{M}^*)^{-1} + \mathscr{R}_{2B} - \mathscr{R}^{\infty}_{2B}. \tag{2.45}$$

Note that $\mathscr{R}_{2B} - \mathscr{R}^{\infty}_{2B}$ may be added without convergence problems because terms through the conditionally convergent mean-field quadrupole are already included in $\mathscr{M}^*$.

This completes the development of our method for dynamically simulating infinite suspensions of hydrodynamically interacting particles. All non-convergent interactions are rigorously included via the Ewald summation technique, and near-field interactions are conveniently included in a pairwise additive fashion via the resistance matrix; for indeed, lubrication interactions are pairwise. Durlofsky *et al.* showed that this procedure of including lubrication is remarkably accurate for any configuration of a finite number of particles. We shall show in the next section that equally good accuracy is obtained for infinite systems.

3. Results

In this section we shall present results that show that the method we have developed is both accurate and computationally efficient. Since the nature of the problem we are addressing is the many-body interactions, comparisons must be made with infinite suspensions. The only known exact solutions are for spatially periodic suspensions, and our comparisons will be with the results of Saffman (1973) and Zick & Homsy (1982) for the sedimentation and permeability problems, and Zuzovsky *et al.* (1983) and Nunan & Keller (1984) for the viscosity problem. We shall see that, in certain limits, the method we have developed is not just accurate, but it is exact. In addition to providing a basis for comparison, the spatially periodic results are a convenient check on the correctness of the rather lengthy formulae for the

Ewald-summed mobility interactions. Indeed, we were originally motivated to examine these periodic suspensions in order to provide this check. Application of the method to other, disordered suspensions can be found in Durlofsky & Brady (1987), Brady & Bossis (1988), Brady & Durlofsky (1988), Phillips, Brady & Bossis (1988*a*, *b*).

3.1. *Sedimentation and permeability of cubic arrays*

The average sedimentation velocity, $\langle \boldsymbol{U} \rangle$, is generally defined relative to zero-volume-flux axes, i.e. such that the average suspension velocity is zero, $\langle \boldsymbol{u} \rangle = 0$. The angle brackets defining the average denote a sum over all particles

$$\langle \boldsymbol{U} \rangle \equiv \frac{1}{N} \sum_{\alpha=1}^{N} \boldsymbol{U}^{\alpha}.$$

From the Ewald-summed resistance matrix in (2.43), (which is identical to (2.25)) we have

$$\langle \boldsymbol{U} \rangle = \langle \boldsymbol{R}_{FU}^{*-1} \cdot \boldsymbol{F} \rangle = \langle \boldsymbol{R}_{FU}^{*-1} \rangle \cdot \boldsymbol{F} = \langle \boldsymbol{M} \rangle \cdot \boldsymbol{F}, \tag{3.1}$$

where, for convenience, we have assumed that all particles are identical so that the force $\boldsymbol{F}$ is the same for all. Thus, the sedimentation velocity is an average of the entire mobility matrix $\boldsymbol{M} \equiv \boldsymbol{R}_{FU}^{*-1}$. Note that even though the definition of $\boldsymbol{U}$ includes the rotational velocities and that of $\boldsymbol{F}$ includes the torques, since we assume that the torque on each particle is identically zero for sedimentation, (3.1) relates the average translational velocity to the force.

The permeability, $\boldsymbol{K}$, of a porous medium or a fixed bed of particles is usually defined as the proportionality between the average pressure gradient and the average velocity when the particles are fixed in space, i.e. through Darcy's law:

$$\nabla \langle p \rangle = -\eta \boldsymbol{K}^{-1} \cdot \langle \boldsymbol{u} \rangle. \tag{3.2}$$

Since the pressure gradient is related to the average force through the macroscopic hydrostatic balance (2.16), we have for the 'resistivity', $\boldsymbol{K}^{-1}$, from (2.43)

$$\boldsymbol{K}^{-1} = n \langle \boldsymbol{R}_{FU}^{*} \rangle. \tag{3.3}$$

The resistivity is the average of the entire resistance matrix $\boldsymbol{R}_{FU}^{*}$. From our definition, one must remember to average only the translational velocity/force components of $\boldsymbol{R}_{FU}^{*}$ to obtain the conventional permeability. If the microstructure of the porous medium had a handedness or chirality, the couplings in $\boldsymbol{R}_{FU}^{*}$ between the torque and the translation velocity would give the average torque required to keep the medium from rotating in the uniform flow (cf. Koch & Brady 1987).

From (3.1) and (3.3) we see that the sedimentation velocity and permeability are closely related. The significant difference, apart from the simple scaling factor n, is the commutation of the inversion operator and the average; for the sedimentation velocity, the resistance matrix is inverted and then averaged, while for the permeability, the resistance matrix is averaged and then inverted. In general, these operations do not commute, and the sedimentation velocity and permeability are quite different. The physics of the particle interactions is also quite different in the two cases, with the interactions being screened in a porous medium. For a spatially periodic lattice however, the sedimentation velocity and permeability are simply related; since all particles are identical in a periodic lattice, no averaging is necessary, and therefore averaging and inverting commute.

In figure 1 we show a comparison of the non-dimensional sedimentation velocity

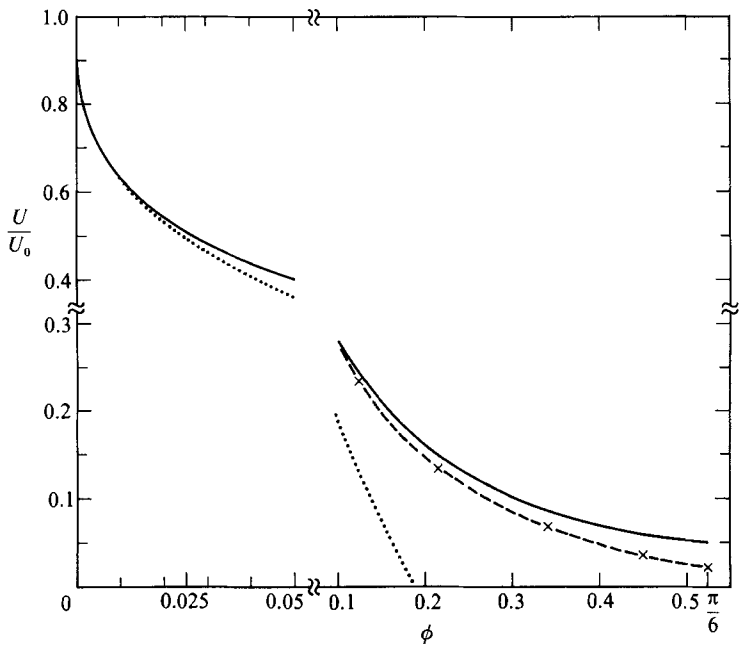

FIGURE 1. Non-dimensional sedimentation velocity of a simple cubic array of spheres as a function of volume fraction ϕ. The solid curve is the result of the Stokesian-dynamics method, the dashed curve is the exact result of Zick & Homsy (1982), and the dotted curve is the point-force solution of Saffman (1973). To facilitate comparison at high and low ϕ, the ordinate and abscissa scales change for $\phi \geqslant 0.1$. The exact and Stokesian-dynamics results are indistinguishable up to $\phi = 0.1$.

of a simple cubic array of spheres obtained by our Stokesian-dynamics simulation method with the calculations of Saffman and Zick & Homsy. The figure has been split into low- and high-ϕ regions in order to clearly display the results. Saffman's calculations are for point-force particles only and result in a sedimentation velocity $U/U_0 = 1 - 1.738\phi^{\frac{1}{3}}$, where U_0 is the Stokes settling velocity of an isolated sphere. At low ϕ all calculations agree, and in fact the Ewald-summed mobility interactions for point forces given in (2.39) are *identical* to Saffman's calculations. That is, Ewald summing the Green function $\boldsymbol{J}$ exactly reproduces Hasimoto's (1959) solution for the spatially periodic Stokes' Green function.

We see in figure 1 that when extended to higher ϕ the point-force solution gives a very poor estimate of the sedimentation velocity and predicts a *negative* sedimentation rate for $\phi > 0.19$. This is a rather catastrophic failure and also indicates that the mobility matrix formed from point forces has lost positive definiteness. Including the finite size of the particles – that is, retaining the $\frac{1}{6}a^2\nabla^2\boldsymbol{J}$-terms that come from the quadrupole $\boldsymbol{Q}'$ in (2.24) and from Faxén's law – completely removes this aphysical behaviour and gives reasonable sedimentation velocities.

There is actually a very close correspondence between our method and the one used by Zick & Homsy, Zick & Homsy solved the integral equation for Stokes' flow for the periodic suspension using Hasimoto's periodic Green function. Instead of discretizing the surface of the particle, they too expanded the force density on the particle's surface in moments. The zeroth moment corresponds to assuming the force density is constant over the particle surface. A constant force density on a sphere surface is equivalent to a point force plus the quadrupole term, $\frac{1}{6}a^2\boldsymbol{FI}$, of equation (2.24) at the sphere centre. Thus, Zick & Homsy's zeroth-order method is identical

ϕ	PF	$\langle \boldsymbol{M}^*_{UF} \rangle$	$\langle \boldsymbol{M}^*_{UF} \rangle_Q$	$\langle \boldsymbol{R}^{*-1}_{FU} \rangle$	Z & H
0.001	0.8262	0.8250	0.8250	0.8249	0.8251
0.027	0.4787	0.4990	0.4988	0.4975	0.4980
0.064	0.3049	0.3600	0.3591	0.3574	0.3559
0.125	0.1312	0.2450	0.2418	0.2410	0.2330
0.216	−0.04261	0.1599	0.1506	0.1496	0.1344
0.343	−0.2164	0.1109	0.08738	0.08689	0.06494
0.45	−0.3316	0.1012	0.06071	0.06042	0.03559
0.5236	−0.4001	0.1050	0.05012	0.04990	0.02375

TABLE 1. Comparison of the various levels of approximation for the sedimentation velocity of a simple cubic array of spheres as a function of volume fraction ϕ. PF refers to the point-force result of Saffman (1973); $\langle \boldsymbol{M}^*_{UF} \rangle$ is the Ewald-summed mobility matrix including the finite size of the particles; $\langle \boldsymbol{M}^*_{UF} \rangle_Q$ is the same as $\langle \boldsymbol{M}^*_{UF} \rangle$ except that the mean-field quadrupole contribution is also included; $\langle \boldsymbol{R}^{*-1}_{FU} \rangle$ is the same as $\langle \boldsymbol{M}^*_{UF} \rangle_Q$, except that the two-body lubrication effects are included via (2.45); Z & H are the exact results of Zick & Homsy (1982).

to our $\langle \boldsymbol{M}^*_{UF} \rangle$ without the mean-field quadrupole (2.29). (The angle brackets are used here to denote an average, although they are not necessary for the periodic problem.) Comparison of our results with those in table 1 of Zick & Homsy, where they discuss the accuracy of their method as a function of the number of moments used and the volume fraction, shows agreement to all significant figures of $\langle \boldsymbol{M}^*_{UF} \rangle$ and their zeroth-order method.

The inclusion of the mean-field quadrupole in our method, which we shall denote as $\langle \boldsymbol{M}^*_{UF} \rangle_Q$, reproduces quite well Zick & Homsy's second-order method, which includes the complete quadrupole interactions – that is, including terms through equation (2.28). Note that for a cubic lattice there is no coupling between even and odd moments of the force density, so the torque and stresslet terms in (2.25)–(2.28) or in the grand mobility or resistance matrices, (2.42) and (2.44), have no effect on the sedimentation velocity. Specifically, from their table 1 for a simple cubic lattice at the maximum volume fraction, $\phi_{\max} = 0.5236$, we have $\langle \boldsymbol{M}^*_{UF} \rangle_Q = 0.05012$ compared to their value of 0.03566. (For the BCC and FCC lattices the comparisons are: BCC, $\phi = 0.6802$: 0.01184 *vs.* 0.01161, and FCC, $\phi = 0.7405$: 0.009824 *vs.* 0.007360, where the first number is ours and the second Zick & Homsy's. In general, the agreement between the Stokesian-dynamics results and the sedimentation velocity for the BCC and FCC lattices is the same as that shown in figure 1 for the SC lattice.) Thus, our mean-field quadrupole term reproduces quite well the complete quadrupole interaction.

In table 1 we show a detailed comparison of the effect of various levels of hydrodynamic approximation on the sedimentation velocity of a simple cubic lattice as a function of volume fraction. One sees an improvement in going from point forces (PF) to point force plus finite size ($\langle \boldsymbol{M}^*_{UF} \rangle$), and a further improvement in including the mean-field quadrupole ($\langle \boldsymbol{M}^*_{UF} \rangle_Q$). However, including lubrication in the resistance matrix ($\langle \boldsymbol{R}^{*-1}_{FU} \rangle$) through (2.45) makes almost no improvement over the mean-field quadrupole. (It should be noted that, when including the near-field lubrication interactions in (2.45), the sum is performed over all particles in the lattice, i.e. a convergent sum over an infinite number of particles.) The reason that lubrication has virtually no effect on sedimentation velocities is because the fluid displaced by the falling particles flows up through the interstices of the lattice and not through the small gaps between particles. There are no singular force densities

generated by the flowing fluid on the particle surfaces, the sedimentation velocity and permeability both approach non-zero values as $\phi \to \phi_{\max}$ (the resistance matrix $\boldsymbol{R}^*_{FU}$ is not singular in this limit) and lubrication plays no role. This is true for sedimentation whether the suspension is ordered or disordered (Brady & Durlofsky 1988). For the viscosity problem to be discussed next, however, lubrication forces do play a vital role.

While it is clear physically why there is no singular behaviour in sedimentation to be captured by lubrication, the fact that including the exact two-body resistance interactions has no effect is actually much more revealing about the nature of many-body interactions in sedimentation. An examination of table 1 of Zick & Homsy shows that in order to obtain 10% accuracy at $\phi_{\max}$ for the simple cubic lattice one must include up to the fourth moment – that is, monopoles, dipoles, quadrupoles, octupoles *and* hexadecapoles. (For comparable accuracy at $\phi_{\max}$ in BCC though the sixth moment is needed, while for the FCC the eighth moment is needed!) The interactions we add in the resistance matrix include contributions from all moments, but from only two bodies because they are added pairwise. Thus, it is the many-body hexadecapoles for the simple cubic lattice (and the many-body fourth, sixth and eighth moments for BCC and FCC) that give the additional contribution to the sedimentation velocity.

For regular arrays, the symmetry of the lattice can be exploited to drastically reduce the number of unknowns, specifically Zick & Homsy find the number of unknowns is given by $\frac{1}{8}(M+2)(3M+4)$, where M is the number of moments retained. In a disordered suspension, however, not only can one not exploit any symmetries to reduce the number of unknowns per moment, but one also needs N particles, rather than only one. Considering the fact that including the complete quadrupole rather than only the mean-field increases the number of unknowns from $11N$ to $26N$, resulting in a 13-fold increase in computation time for an insignificant improvement in accuracy, it is doubtful that any more moments can (or should) be included in the grand mobility matrix. In a dynamic simulation, where the interactions must be updated because particle positions have changed, these restrictions become even more severe.

3.2. *Shear viscosity of cubic arrays*

Although lubrication played no role in the sedimentation velocity and permeability, it is essential for the shear viscosity of concentrated suspensions. To calculate the shear viscosity, we need the relationship between the bulk stress and the imposed rate of strain. From (2.11) we see that the particle contribution to the bulk stress is given by $-n\langle \boldsymbol{S} \rangle$. (For spherical particles in a linear shear flow there are no antisymmetric stresses and $\mathscr{L}_{ij} = 0$.) The average particle stresslet is related to the bulk rate of strain $\langle \boldsymbol{e} \rangle$ by a fourth-order tensor $\boldsymbol{A}$:

$$\langle \boldsymbol{S} \rangle = -\boldsymbol{A} : \langle \boldsymbol{e} \rangle, \tag{3.4}$$

where the tensorial 'viscosity' from (2.44) is given by

$$\boldsymbol{A} = \langle \boldsymbol{R}^*_{SU} \cdot \boldsymbol{R}^{*-1}_{FU} \cdot \boldsymbol{R}^*_{FE} - \boldsymbol{R}^*_{SE} \rangle. \tag{3.5}$$

Here, we are considering force- and torque-free particles. In general, there may be additional contributions to the bulk stress due to interparticle forces or Brownian motion, but these pose no convergence problems for stresses or velocities, and they may be simply added to the bulk stress. The stress $\langle \boldsymbol{\sigma} \rangle$ appearing in (2.4) is the

hydrodynamic, or contact, stress due to the fluid velocity gradient on the particle surfaces (cf. Batchelor 1977; Brady & Bossis 1988).

Following Zuzovsky *et al.* and Nunan & Keller, the symmetry of the cubic lattice allows us to write

$$A_{ijlk} = \eta(1+\beta)\tfrac{1}{2}(\delta_{ik}\delta_{jl}+\delta_{il}\delta_{jk}-\tfrac{2}{3}\delta_{ij}\delta_{kl})+\eta(\alpha-\beta)(\delta_{ijkl}-\tfrac{1}{3}\delta_{ij}\delta_{kl}), \tag{3.6}$$

where δ_{ijkl} is one if all subscripts are the same and zero otherwise. α and β are functions of the lattice geometry and the volume fraction. One should also note that in a cubic lattice $\boldsymbol{U}-\langle\boldsymbol{u}\rangle \equiv 0$, i.e. $\boldsymbol{R}^{*-1}_{FU}\cdot\boldsymbol{R}^{*}_{FE} = 0$ and the particles move at the velocity of the bulk shear flow, so that the only term contributing in (3.5) is $\boldsymbol{R}^{*}_{SE}$. Again, the even and odd moments do not couple, so we only need concern ourselves with $\langle\boldsymbol{M}^{*-1}_{ES}\rangle$ and $\langle\boldsymbol{R}^{*}_{SE}\rangle$. The distinction between the mobility and resistance matrices is to imply without and with lubrication, respectively. It should also be noted that we are calculating the viscosity for a single, instantaneous configuration of the periodic array, and not a time average.

In figure 2(*a*, *b*) we compare the α- and β-functions for a simple cubic lattice obtained by our Stokesian-dynamics method, $\langle\boldsymbol{R}^{*}_{SE}\rangle$, with the exact results of Nunan & Keller as a function of volume fraction. Nunan & Keller used the same method as Zick & Homsy for solving the integral equation with the spatially periodic Green function. Their numerical solutions are the dashed curves and terminate at the valves of ϕ indicated in the figures. At higher ϕ, more moments are needed to obtain convergence, and they report that α for an SC lattice at $\phi = 0.49$ was not converged even for $M = 13$ (cf. their table 1). At dilute ϕ, again the Ewald-summed mobility matrix $\boldsymbol{M}^{*}_{ES}$ is exact, and its invert (the dotted curve in the figures) reproduces α and β correct to $O(\phi^{\frac{8}{3}})$ (cf. equations (110) and (111) of Zuzovsky *et al.*). In contrast to sedimentation, however, as $\phi \to \phi_{\max}$ lubrication forces are important in the viscosity because of the relative motion of adjacent particles in the cubic lattice. The lubrication singularities are only two-body effects, and thus our method reproduces the exact behaviour as $\phi \to \phi_{\max}$; specifically, $\alpha \sim \frac{3}{16}\pi\epsilon^{-1}-\frac{27}{8}\pi\ln\epsilon+\ldots$ and $\beta \sim -\frac{1}{4}\pi\ln\epsilon+\ldots$ as $\epsilon = 1-(\phi/\phi_{\max})^{\frac{1}{3}} \to 0$, which are the dot-dashed curves in the figures. The good agreement over the whole range of ϕ results from the fact that our method is exact for low and high ϕ, and therefore the curve has little room for variation at intermediate values of ϕ.

Our results give the exact singular behaviour as $\epsilon \to 0$; the first error lies in the $O(1)$ constant associated with the asymptotic forms. Our $O(1)$ constants are a combination of $(\boldsymbol{M}^{*}_{ES})^{-1}$ and the order-one term in the two-body lubrication singularities. There is no reason for our $O(1)$ constants to be exact, but judging from the figures, particularly the $\ln\epsilon$ singular function SC β, they appear to be quite reasonable. The worst agreement between our results and those of Nunan & Keller are for the FCC β (not shown). Nunan & Keller reported significant difficulty in obtaining convergence with increasing number of moments for this function and an inability to match the $O(1)$-terms in the singular behaviour of β with their numerical results. It is not known whether the difference seen in our results is real or if there is some inaccuracy in the calculations of Nunan & Keller.

3.3. *Spin viscosity of cubic arrays*

The last example we present is the spin viscosity of cubic lattices. The spin viscosity is the relationship between the average torque $\langle\boldsymbol{L}\rangle$ and the average angular velocity $\langle\boldsymbol{\omega}\rangle$. It arises in constitutive equations for antisymmetric stresses, the principal application being ferrofluids (Zuzovsky *et al.*; Rosensweig 1988). From (2.11) we see

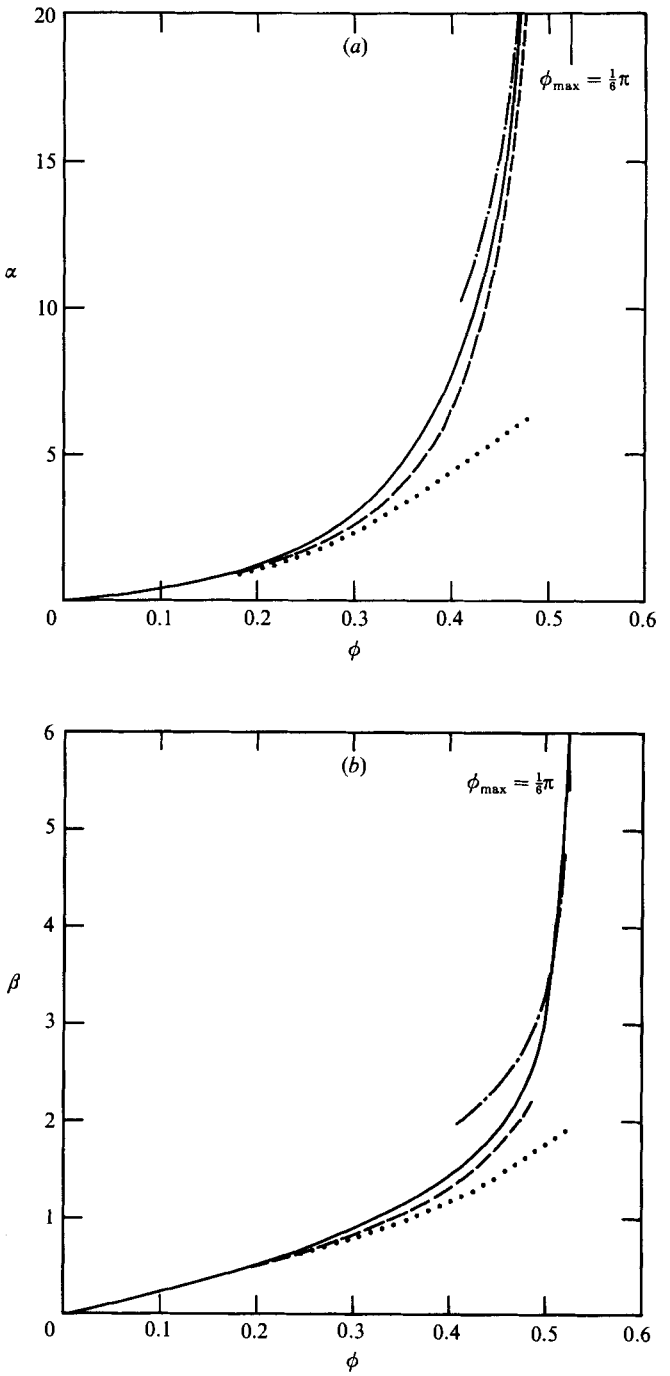

FIGURE 2. The shear viscosity functions (*a*) α and (*b*) β defined in (3.6) for a simple cubic array as a function of volume fraction. The solid curves are the Stokesian-dynamics results, the dashed curves are the exact solutions of Nunan & Keller (1984), which terminates at $\phi = 0.48$, the dotted curves are the far-field results obtained from $\langle \boldsymbol{M}_{\boldsymbol{ES}}^{*-1} \rangle$, i.e. no lubrication, and the dot-dashed curves are the singular form as $\phi \to \phi_{max}$.

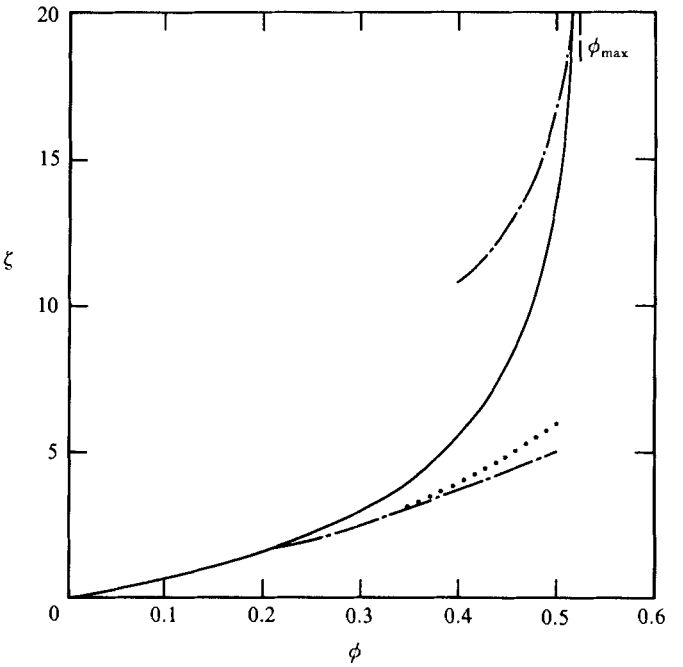

FIGURE 3. The spin viscosity function ζ defined in equation (3.9) for the SC lattice as a function of volume fraction. The solid curve is the Stokesian-dynamics results, the dotted curve is the far-field results obtained from $\langle \boldsymbol{M}_{\Omega L}^{*-1} \rangle$, and the dot-dashed curves are the asymptotic forms as $\phi \to \phi_{\max}$ and as $\phi \to 0$.

that the particle contribution to the antisymmetric part of the bulk stress is $-n\langle \mathscr{L} \rangle = -n\boldsymbol{\varepsilon} \cdot \langle \boldsymbol{L} \rangle$. The average torque is related to the bulk angular velocity by

$$\langle \boldsymbol{L} \rangle = -\boldsymbol{B} \cdot \langle \boldsymbol{\omega} \rangle, \tag{3.7}$$

and from the grand resistance matrix (2.44)

$$\boldsymbol{B} = \langle \boldsymbol{R}_{L\Omega}^{*} \rangle, \tag{3.8}$$

where $\boldsymbol{R}_{L\Omega}^{*}$ is the submatrix of $\boldsymbol{R}_{FU}^{*}$ that couples torque and angular velocity. The symmetry of the cubic lattice allows us to write

$$B_{ij} = \zeta \delta_{ij}, \tag{3.9}$$

where the scalar function ζ depends on the lattice and the volume fraction.

In figures 3 and 4 we show the results for the spin viscosity function ζ as a function of ϕ for the three cubic lattices SC, BCC and FCC. ζ has not yet been computed exactly for all ϕ, but high- and low-ϕ asymptotes are known and can be found in Zuzovsky *et al.* Again, the Stokesian dynamics results are exact in the low-ϕ limit, being correct to $O(\phi^2)$ (cf. equation (112) of Zuzovsky *et al.*), and in the high-ϕ limit, where $\zeta \sim \ln \epsilon$ for all three lattices, with a coefficient depending on the number of near neighbours.

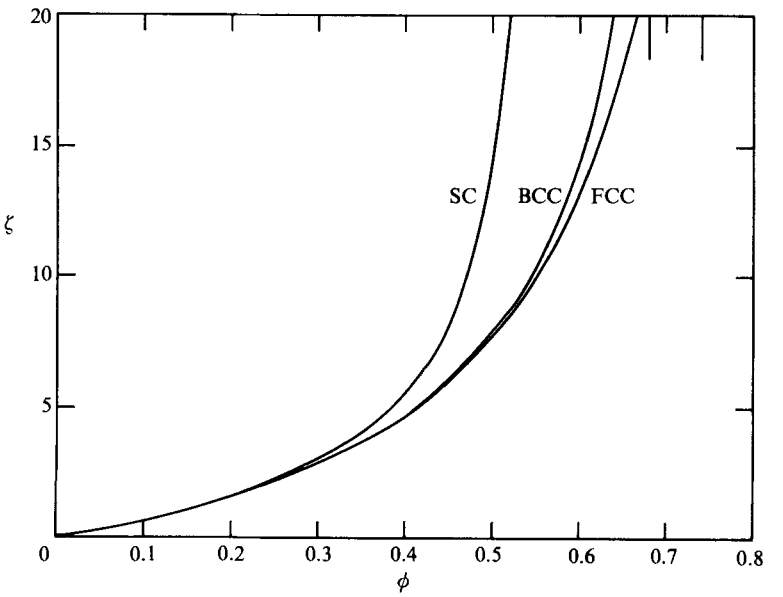

FIGURE 4. Comparison of the spin viscosity function ζ for SC, BCC and FCC lattices.

4. Conclusions

In this paper we have presented a general and rigorous method for calculating hydrodynamic interactions in infinite suspensions. While mathematically involved, the method developed in §2 yields a very simple and intuitive result: since the hydrodynamic interactions are purely geometric, they are the same whether or not divergences occur. The particles do not know if their forces sum to zero or to a finite average; the interactions must be the same in both cases. One need not follow any of the mathematical analysis to understand this basic result. The method allows the entire range of suspension problems to be studied, from self-diffusion to sedimentation to rheology to flow in porous media, with no change in formulation or procedure. Further, the same formulation applies whether the microstructure is ordered or disordered. The only limitations of the method are of a computational nature, involving the number of moments used in the expansion of the force density on the particle surfaces in the construction of the grand mobility matrix and the number of particles used in a periodic cell. By increasing both of these the method can be made arbitrarily accurate. Just how many moments or particles are needed to accurately model an infinite disordered suspension depends on the property studied and is discussed in detail in Phillips *et al.*

It should also be appreciated that it is not necessary to expand the force density on the particle surfaces in moments for the convergence procedure to work. One could solve directly the integral equations (2.25), etc. by discretizing the surfaces of the particles and Ewald summing all the point-force propagators. While this method would work, it is not clear that one could obtain equivalent accuracy with the same number of unknowns per particle as with our moments expansion. Recall that our method requires 11 unknowns per particle. Another advantage of the moments expansion is that it maintains precisely all symmetry properties of the particle interactions, regardless of the accuracy of the calculations and the configuration of

the particles. Guaranteeing such symmetry when discretizing the integral equation would be extremely difficult, if not impossible. From a computational point of view, filling the mobility matrix, even with the Ewald sums, is an $O(N^2)$ operation. Inverting the mobility matrix to include lubrication is generally the most costly step, requiring $O(N^3)$ operations, but it appears at present that this is a more economical method than solving directly the integral equation.

In this paper we have applied our Stokesian-dynamics method to the simplest suspension problems – spatially periodic ones. It should be noted that the good accuracy we have obtained with our method for periodic suspensions comes at far less computational cost than the calculations of either Zick & Homsy or Nunan & Keller. Indeed, in both the sedimentation and viscosity problems, the symmetry could be exploited so that we only had one unknown. The results could be obtained by Ewald summing and adding lubrication; the matrix inversions could be done by hand. By contrast, Zick & Homsy and Nunan & Keller had to solve large equation sets to obtain their results. This computational advantage becomes even greater when one moves to disordered suspensions and to dynamic simulation.

Several applications of our Stokesian-dynamics method to disordered systems have already appeared (Durlofsky & Brady 1987; Brady & Bossis 1988; Phillips *et al.* 1988*a*, *b*) and several more are in progress. In our earliest simulations (Bossis & Brady 1984; Brady & Bossis 1985) we restricted our studies to sheared monolayer suspensions – that is, three-dimensional spherical particles lying in the same plane. We chose this system not only because the number of degrees of freedom is reduced (from $11N$ to $6N$), but also because many of the divergence problems disappear for monolayer suspensions. In particular, all moments beyond the monopole (forces) are absolutely convergent for a monolayer, and we only studied systems in which the average force was zero, thereby avoiding the convergence problems. One indication that this procedure is correct is that our mobility and/or resistance matrices never lost positive definiteness; the other is that recent calculations employing the full Ewald sums gave statistically the same results.

The method we have developed here for the Stokes' equations should also find application in other problems that display the same combination of far- and near-field physics. There is a very close similarity between the Stokes problem and the electrostatic problem, the latter being governed by Laplace's equation, and an even closer similarity with the equations of linear elasticity. The Stokesian dynamics method can be and has been applied (Bonnecaze 1987) to Laplace-governed problems with accuracy equal to that shown here. Stokesian dynamics also finds use in a variety of problems other than sedimentation and viscosity; the interested reader is referred to the review article (Brady & Bossis 1988) for an indication of the types of problems that can be studied by this method.

We would like to thank our colleague L. Durlofsky for many useful discussions concerning Stokesian dynamics. The work was supported in part by the Centre National pour la Recherche Scientifique and by the National Science Foundation under grants CBT-8696067 and INT-8413695. Computer time was provided by Centre de Calcul Vectoriel pour la Recherche and by the San Diego Supercomputer Center. R.J.P. would also like to acknowledge the support of an NSF fellowship.

REFERENCES

ARP, P. A. & MASON, S. G. 1977 The kinetics of flowing dispersions. VIII. Doublets of rigid spheres (theoretical). *J. Colloid Interface Sci.* **61**, 21–43.

BATCHELOR, G. K. 1970 The stress system in a suspension of force-free particles. *J. Fluid Mech.* **41**, 545–570.

BATCHELOR, G. K. 1972 Sedimentation in a dilute dispersion of spheres. *J. Fluid Mech.* **52**, 245–268.

BATCHELOR, G. K. 1974 Transport properties of two-phase materials with random structure. *Ann. Rev. Fluid Mech.* **6**, 227–255.

BATCHELOR, G. K. 1977 The effect of Brownian motion on the bulk stress in a suspension of spherical particles. *J. Fluid Mech.* **83**, 97–117.

BATCHELOR, G. K. & GREEN, J. T. 1972 The determination of the bulk stress in a suspension of spherical particles to order c^2. *J. Fluid Mech.* **56**, 401–427.

BEENAKKER, C. W. J. 1986 Ewald sum of the Rotne–Prager tensor. *J. Chem. Phys.* **85**, 1581–1582.

BONNECAZE, R. 1987 A method for determining the effective conductivity of dispersions of particles. M.S. thesis, California Institute of Technology, 31 pp.

BOSSIS, G. & BRADY, J. F. 1984 Dynamic simulation of sheared suspensions. I. General method. *J. Chem. Phys.* **80**, 5141–5154.

BOSSIS, G. & BRADY, J. F. 1987 Self-diffusion of Brownian particles in concentrated suspensions under shear. *J. Chem. Phys.* **87**, 5437–5448.

BRADY, J. F. & BOSSIS, G. 1985 The rheology of concentrated suspensions of spheres in simple shear flow by numerical simulation. *J. Fluid Mech.* **155**, 105–129.

BRADY, J. F. & BOSSIS, B. 1988 Stokesian dynamics. *Ann. Rev. Fluid Mech.* **20**, 111–157.

BRADY, J. F. & DURLOFSKY, L. 1988 On the sedimentation rate of disordered suspensions. *Phys. Fluids* **31**, 717–727.

BRINKMAN, H. C. 1947 A calculation of the viscous force exerted by a flowing fluid on a dense swarm of particles. *Appl. Sci. Res.* **A1**, 27–34.

DICKINSON, E. 1985 Brownian dynamics with hydrodynamic interactions: The application to protein diffusional problems. *Chem. Soc. Rev.* **14**, 421–455.

DURLOFSKY, L. 1986 Topics in fluid mechanics: I. Flow between finite rotating disks. II. Simulation of hydrodynamically interacting particles in Stokes flow. Ph.D. thesis, Massachusetts Institute of Technology.

DURLOFSKY, L. & BRADY, J. F. 1987 Analysis of the Brinkman equation as a model for flow in porous media. *Phys. Fluids* **30**, 3329–3341.

DURLOFSKY, L. & BRADY, J. F. 1988 Dynamic simulation of bounded suspensions. *J. Fluid Mech.* (to appear).

DURLOFSKY, L., BRADY, J. F. & BOSSIS, G. 1987 Dynamic simulation of hydrodynamically interacting particles. *J. Fluid Mech.* **180**, 21–49.

EWALD, P. P. 1921 Die berechnung optischa und elektrostatischer Gitterpotentiale. *Ann. Phys.* **64**, 253–287.

GLENDINNING, A. B. & RUSSEL, W. B. 1982 A pairwise additive description of sedimentation and diffusion in concentrated suspensions of hard spheres. *J. Colloid Interface Sci.* **89**, 124–143.

HASIMOTO, H. 1959 On the periodic fundamental solution of the Stokes equations and their application to viscous flow past a cubic array of spheres. *J. Fluid Mech.* **5**, 317–328.

HINCH, E. J. 1977 An averaged-equation approach to particle interactions in a fluid suspension. *J. Fluid Mech.* **83**, 695–720.

HOWELLS, I. D. 1974 Drag due to the motion of a Newtonian fluid through a sparse random array of small fixed rigid objects. *J. Fluid Mech.* **64**, 449–475.

JEFFREY, D. J. 1973 Conduction through a random suspension of spheres. *Proc. R. Soc. Lond.* **A335**, 355–367.

JEFFREY, D. J. & ONISHI, Y. 1984 Calculation of the resistance and mobility functions for two unequal rigid spheres in low-Reynolds-number flow. *J. Fluid Mech.* **139**, 261–290.

KIM, S. & MIFFLIN, R. T. 1985 The resistance and mobility functions for two equal spheres in low-Reynolds-number flow. *Phys. Fluids* **28**, 2033–2045.

KOCH, D. L. & BRADY, J. F. 1987 On the symmetry properties of the effective diffusivity tensor in anisotropic porous media. *Phys. Fluids* **30**, 642–650.

LADYZHENSKAYA, O. A. 1963 *The Mathematical Theory of Viscous Incompressible Flow.* Gordon & Breach.

LANDAU, L. D. & LIFSHITZ, E. M. 1959 *Fluid Mechanics.* Pergamon.

MAZUR, P. & VAN SAARLOOS, W. 1982 Many-sphere hydrodynamic interactions and mobilities in a suspension. *Physica* **115A**, 21–57.

NUNAN, K. C. & KELLER, J. B. 1984 Effective viscosity of a periodic suspension. *J. Fluid Mech.* **142**, 269–287.

O'BRIEN, R. W. 1979 A method for the calculation of the effective transport properties of suspensions of interacting particles. *J. Fluid Mech.* **91**, 17–39.

PHILLIPS, R. J., BRADY, J. F. & BOSSIS, G. 1988*a* Hydrodynamic transport properties of hard-sphere dispersions. I. Suspensions of freely mobile particles. *Phys. Fluids* (to appear).

PHILLIPS, R. J., BRADY, J. F. & BOSSIS, G. 1988*b* Hydrodynamic transport properties of hard-sphere dispersions. II. Porous media. *Phys. Fluids* (to appear).

ROSENSWEIG, R. E. 1988 *Ferrohydrodynamics.* Cambridge University Press.

RUBINSTEIN, J. 1986 Effective equations for flow in random porous media with a large number of scales. *J. Fluid Mech.* **170**, 379–383.

SAFFMAN, P. G. 1973 On the settling speed of free and fixed suspensions. *Stud. Appl. Maths.* **52**, 115–127.

SMITH, E. R., SNOOK, I. K. & VAN MEGEN, W. 1987 Hydrodynamic interactions in Brownian dynamics I. Periodic boundary conditions for computer simulations. *Physica* **143A**, 441–467.

ZICK, A. & HOMSY, G. M. 1982 Stokes flow through periodic arrays of spheres. *J. Fluid Mech.* **115**, 13–26.

ZUZOVSKY, M., ADLER, P. M. & BRENNER, H. 1983 Spatially periodic suspensions of convex particles in linear shear flows. III. Dilute arrays of spheres suspended in Newtonian fluids. *Phys. Fluids* **26**, 1714–1723.